MAGNET DEVELOPMENT FOR SPring-8 UPGRADE

T. Watanabe†, T. Aoki, H. Kimura, S. Takano, T. Taniuchi, K. Tsumaki, K. Fukami, S. Matsubara, C. Mitsuda, Japan Synchrotron Radiation Research Institute (JASRI), Hyogo, Japan
T. Hara, RIKEN, Hyogo, Japan

Abstract

Major upgrade of SPring-8 is being planned, aiming at next generation light source [1, 2]. One of features for newly designed magnets for the upgrade is a permanent magnet based dipole magnet for substantial energy saving [3, 4]. The new dipole magnets have been designed to be equipped with (i) a field variable function by mechanically controlling magnetic flux into a beam axis, (ii) a nose structure on iron poles for smooth magnetic field transition in its longitudinal gradient field, and (iii) a nearly zero temperature coefficient by specifically designed magnetic circuits. Demagnetization due to radiation is also a critical issue and has been studied. Although electromagnet based multi-pole magnets are rather conventional technologies, yet the new magnets need to be designed to fit in a high packing factor lattice. Magnet alignment is as well a key issue in order to secure adequate dynamic apertures. Current designs and recent progress in the magnet developments are presented.

PERMANENT MAGNET BASED DIPOLE MAGNETS

One of underlying concepts for the SPring-8 upgrade is to achieve significantly higher brilliance with lower energy consumption [2]. For that, permanent magnet (PM) based dipole magnets have been developed. It would be expected to save a fraction of Megawatt power, or even more.

PMs have been occasionally used for accelerators for a variety of purposes, but still several concerns have been pointed out when one discusses reliability, stability, or usability of such magnets [3-5]:

1. Magnetic field adjustability
2. Temperature dependence of magnet materials
3. Demagnetization

Other details, such as field quality, fringe field, specific field distributions like so-called longitudinal gradient field, and manufacturing cost, should also be verified in order to build a robust and reliable accelerator.

At SPring-8, we have investigated above issues through research-and-development (R&D) to make sure of a feasibility of PM for SPring-8-II. In the paper, we summarize the progress in the R&D.

Magnetic Field Adjustability

Remotely controlled magnetic field adjustability may not be necessary, especially for dipole magnets. However, some amount of field adjustability is still demanded, because it could help adjust the magnetic field in an initial tuning of magnets, and compensate for demagnetization in a long time range.

We have proposed and demonstrated a field adjustable magnetic circuit, in which a portion of magnetic flux generated by PM was intentionally leaked out of a closed loop for beam axis. Hence a flux density on a beam axis can be adjusted by changing the portion [3]. In the case, the dynamic range of tuning can be tens of per cent.

Temperature Dependence

Magnetic flux generated by PM, Φ_{PM}, changes as temperature is drifted by ΔT. The ratio, k_{PM}, is in general negative, i.e., the magnetic flux density electrons experience decreases as temperature increases. When some of flux, Φ_{shunt}, is shunted in a magnetic circuit, the flux on a magnetic gap, Φ_{gap}, is expressed as

$$\begin{aligned}\Phi_{gap} &= \Phi_{PM} - \Phi_{shunt} \\ &= \left(1 + k_{PM}\Delta T\right)\Phi^0_{PM} - \left(1 + k_{shunt}\Delta T\right)\Phi^0_{shunt}\end{aligned}, \quad (1)$$

where k_{shunt} is the temperature coefficient of the shunt circuit, and Φ^0_{PM} and Φ^0_{shunt} are initial magnetic flux respectively for PM and the shunt circuit. Thus, the temperature dependence can be compensated by controlling the magnetic flux as;

$$\frac{\Phi^0_{shunt}}{\Phi^0_{PM}} = \frac{k_{PM}}{k_{shunt}}. \quad (2)$$

In commercial based PM, Fe-Ni alloy has been employed as the shunt material having the well-defined temperature coefficient k_{shunt}.

A C-shaped hybrid-type dipole magnet has been fabricated and the compensation scheme was tested. The result was obtained as indicated in Fig.1. Red dots in Fig.1 show normalized magnetic field *B* without compensation for a temperature range from 20 to 30 degree Celsius. One can see that the magnetic field on a gap decreases as the temperature increases. The temperature coefficient, k_{PM}, is estimated to be 7.0 x 10^{-4}. When the proper thickness of the shunt alloy is chosen to satisfy Eq.(2), magnetic field on a gap is invariant for temperature drift as presented in blue squares in Fig.1. It follows that the right thickness of Fe-Ni alloy is 18 mm, and when the thickness is not

† twatanabe@spring8.or.jp

ISBN 978-3-95450-147-2

enough like 10 mm, the temperature dependence is not completely compensated (Green in Fig.1). Note that error bars in the magnetic field measurement are negligibly small, since the measurement was done for a static magnetic field generated by PM.

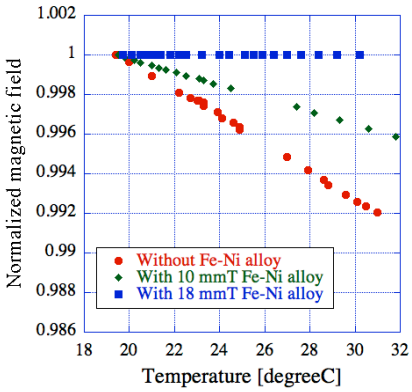

Figure 1: Measurement result of temperature dependence of a C-shaped dipole magnet.

Demagnetization

PM is demagnetized as time elapsed, and also when radiation hits the magnets [5-7]. Demagnetization of undulators due to radiation have been observed at several facilities, and the effects have been studied by hitting PM by electrons, neutrons, or X-ray (e.g., see Ref.[6, 7]). However, it should be noted that conditions for the previous observations and studies are different from our case for dipole magnets in several aspects. First, the permeance coefficient, the ratio of magnetic flux density B and magnetic field strength H at the operation point (see Eq. (3)), for a dipole magnet is normally higher than that for undulator.

$$P_c = -\frac{1}{\mu_0}\frac{B}{H}. \qquad (3)$$

According to 3-dimensional numerical calculation, the permeance coefficient for our dipole magnets are somewhere around 5 to 10, while that for a typical undulator can partially be less than 0.1. It implies that even if exactly the same PM material is used for an undulator and a dipole magnet, the resistance to the radiation should be quite different. Second, some of undulators that have experienced demagnetization are in-vacuum type, but dipole magnets for SPring-8-II are all out-of-vacuum and there are Iron poles in addition to SUS vacuum chambers between magnets and electron paths. Third, Samarium-Cobalt (SmCo) magnet, especially Sm_2Co_{17}, is known to have a high temperature resistance than Neodynium-Iron-Baron (NdFeB) magnets. Even though it is normally required to use NdFeB for an undulator for its high maximum energy product $(BH)_{max}$, one can afford to have an option to use SmCo for a dipole magnet [5]. We are planning to choose Sm_2Co_{17} for SPring-8-II, and demagnetization study of NdFeB and SmCo magnets is underway.

Other Issues

For SPring-8-II, what we call longitudinal gradient bends are planned to be installed so that electrons are to be bent in a large angle when dispersion is small, and are bent in a small angle when dispersion is large. In our case, a single bending magnet is split into three segments with different dipole fields for generating a three-step field distribution [1]. As discussed in Ref. [4], when three segments are placed too close, magnetic cross talk between segments deteriorates the field gradient, and a resulting gradient may be insufficient for the requirement. Once the segments are separated too far, on the other hand, field 'dips' are excited between segments. In order to overcome the trade-off, we have proposed to add a nose structure on Iron poles as illustrated in Fig. 2 [4]. In the case, magnetic field in a longitudinal axis is expected to form a smooth transition from one segment to another. It was experimentally verified as shown in Fig. 3 that measured magnetic field distribution (red open circle) had no more field dips as expected by the simulation (blue solid line). Note that material characteristics in the simulation, such as the remance of magnet B_r, are slightly adjusted so that the absolute strength of simulated magnetic field is briefly consistent with the measurement.

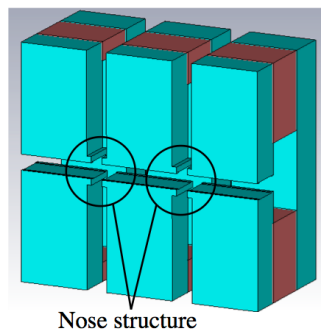

Figure 2: Longitudinal gradient bend with nose structure.

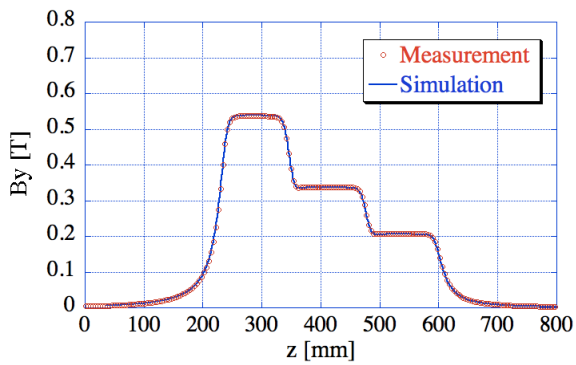

Figure 3: Longitudinal *By* distribution; measurement vs simulation.

Remaining issues, e.g., a field quality, field fringe, and manufacturing costs, have been studied and discussed [3, 4], but are not discussed in the paper due to limited space.

ISBN 978-3-95450-147-2

ELECTROMAGNET BASED MULTI-POLE MAGNETS

Each unit cell has 20 quadrupole and 8 sextupole magnets in addition to octupole and steering magnets [8]. Main parameters are listed in Table 1. One of the features is that the field gradients are all moderate so that the magnets are supposed to be manufactured with existing technologies. A good field region is defined as the region in which the field gradient homogeneity is 10^{-3} or less. Pole edges of quadrupole and sextupole magnets are shimmed to keep the good field region of ±8 mm for quadrupole and ±6 mm for sextupole magnets. Cores are made of laminated steel. All the multi-pole magnets are water-cooled type. The current density of hollow conductors made of oxygen-free copper is less than 3.1 A/mm^2 to suppress the power loss. Total power loss is estimated to be 1.2 MW for normal operation. To prevent interference between coil ends of magnets and other equipment, magnetic poles are tapered in the longitudinal direction. Some sextupole magnets are wound an auxiliary coil to add steering functions. Additionally, independent horizontal and vertical steering magnets are prepared.

Table 1: Main Parameters of Multi-pole Magnets

Parameter	Quadrupole	Sextupole
Bore dia.	34 mm	36 mm
Max gradient	<56 T/m	<2800 T/m^2
Eff. length	200-700 mm	180, 300 mm
Max current	335 A	250 A
Coil turn #	21 turns/pole	9 turns/pole
# magnets	944	352

MAGNET ALIGNMENT

There are mainly two approaches to precisely align magnets. One is to rely on mechanical precision. As next generation light sources make advantages of special magnet, e.g., a combined-function magnet, a straightforward strategy is to manufacture magnets and other apparatus in such a way that magnets can be mechanically aligned. Then a mechanical center of each magnet needs to be well consistent with a magnetic center. Another strategy is to rely on precise magnetic field measurement. We expect it to give better alignment precision than the mechanical alignment. One of such a promising schemes is based on a vibrating wire (VW) method demonstrated by NSLS-II [9]. We plan to employ it to achieve alignment errors of σ~25 μm or less on a girder. Between girders, a conventional laser tracker is supposed to be utilized to achive the errors of σ~45 μm. Figures 4 and 5 are examples of the VW measurement for quadrupole and sextupole magnets. For sextupole magnets, not only (a) By(x) but also (b) Bx(x) gives the magnetic field center in x-axis as presented in Fig. 5. Although in Figs. 4 and 5, the VW method resolves the field center with the precision of sub-μm, total alignment error will be largely influenced by wire sag, kink, temperature dependence of magnet center, and other details. The total evaluation of the VW method is being carried out.

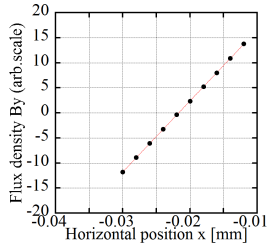

Figure 4: Quadrupole alignment by VW.

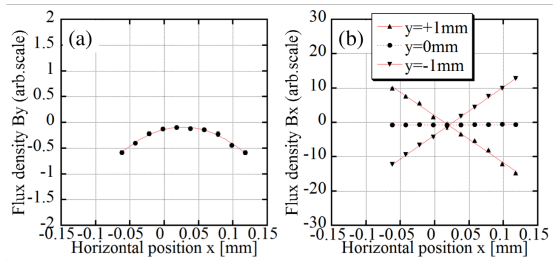

Figure 5: Sextupole alignment by VW. See text in detail.

CONCLUSION

SPring-8 has discussed the major upgrade, SPring-8-II. Features from magnet point of view are permanent magnet based dipole magnets, longitudinal gradient bends, multi-pole magnets with moderate field gradient, etc. So far, nothing has prevented us from proceeding to the next generation light source. In the fiscal year 2017, we plan to build a test cell, or a half cell, to check practical issues like physical interference between components. Parameters and detailed design shown in the paper may change.

REFERENCES

[1] SPring-8-II Conceptual Design Report, Nov. 2014, http://rsc.riken.jp/pdf/SPring-8-II.pdf.

[2] H. Tanaka et al., WEPOW019 in the proceedings.

[3] T. Watanabe et al., Proc. of IPAC2014, Dresden, Germany, p.1253.

[4] T. Taniuchi et al., Proc. of IPAC2015, Richmond, USA, p.2883.

[5] J. Chavanne et al., Proc. of IPAC2015.

[6] T. Bizen et al., Nucl. Instrum. Meth. A 467-468, (2001) p.185.

[7] T. Bizen et al., Nucl. Instrum. Meth. A 515 (2003) p.850.

[8] K. Soutome et al., THPMR022 in the proceedings.

[9] A. Jain et al., Proc. of IWAA2008, Tsukuba, Japan, TU010.

ISBN 978-3-95450-147-2